Advance in Understanding the Biosynthesis of Prostacyclin and Thromboxane A_2 in the Endoplasmic Reticulum Membrane *via* the Cyclooxygenase Pathway

Ke-He Ruan*

The Vascular Biology Research Center and Division of Hematology, Department of Internal Medicine, The University of Texas Health Science Center, Houston, Texas 77030, USA

Abstract: Recent advances in topological and structural characterization of the prostacyclin (PGI_2) and thromboxane A_2 (TXA_2) synthases have led to the understanding of the biosynthesis of PGI_2 and TXA_2 at a structural level. This mini-review focuses on the molecular mechanism of the isomerization of the prostaglandin H_2 to PGI_2 and TXA_2 by their synthases in the endoplasmic reticulum (ER) membrane coordinated with cyclooxygenase-1 or -2. This review summarizes the evidences in which the biosynthesis of PGI_2 and TXA_2 are influenced/modulated by the membrane anchor residues of the synthases and the ER membrane itself, and provides the structural basis for engineering the synthases for the next generation of gene therapy and drug designs targeting the specific synthases.

1. INTRODUCTION

Eicosanoids are a family of bioactive, oxygenated metabolites of polyunsaturated fatty acids. The major eicosanoids synthesized by vascular smooth muscle, endothelium and platelets are prostaglandins and thromboxane [1,2]. These compounds are formed via the "cyclooxygenase" (COX) pathway from arachidonic acid (AA) in three steps [1,3]: (a) stimulus-induced mobilization of AA from membrane phosphoglycerides; (b) conversion of AA to the prostaglandin endoperoxide (prostaglandin H_2 (PGH_2)), by COX; and (c) isomerization of PGH_2 to biologically active end-products prostaglandin D_2 (PGD_2), prostaglandin E_2 (PGE_2), prostacyclin (or called prostaglandin I_2 (PGI_2)) or thromboxane A_2 (TXA_2) by individual synthases in a tissue specific manner [3] (Fig. **1**).

TXA_2, produced from PGH_2 by TXA_2 synthase (TXAS), has been implicated in various pathophysiological conditions as a proaggregatory and vasoconstricting mediator causing thrombosis, stroke and heart attack [4,5]. PGH_2 is also converted to PGI_2 by PGI_2 synthase (PGIS). PGI_2 is the main AA metabolite in vascular walls and has opposing biological properties to TXA_2, representing the most potent endogenous inhibitor of platelet aggregation [6]. PGI_2 is also a strong anti-hypertensive agent through its vasodilatory effect on vascular beds. Thus, it serves as one of the most important cardiovascular protectors. PGIS is mainly present in vascular endothelial cells and smooth muscle cells [7-10]. The PGIS and TXAS genes have been cloned from several sources by our research group and others [11-15]. The two synthases were characterized as cytochrome P450s by optical and EPR spectroscopy, but they lack the monooxygenase activity found in other P450s [16-18]. Like many other membrane-bound mammalian P450s, PGIS and TXAS are both located in the endoplasmic reticulum (ER). As PGI_2 and TXA_2 play important roles in physiological and pathological actions, their productions, in quick response to the biological and pathological changes in the human body by keeping efficient co-ordination of PGIS and TXAS with the up-stream synthase, COX-1 or -2 *in vivo*, are extremely important.

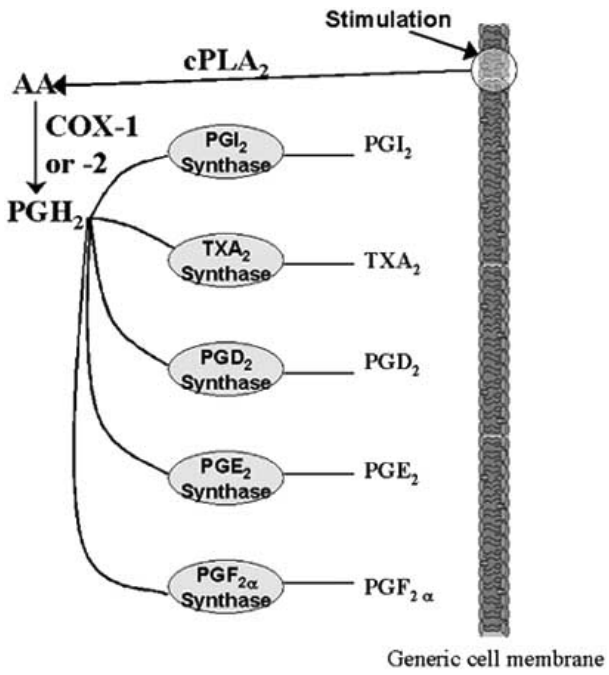

Fig. (1). Biosynthesis of the prostanoids.

In this review, the current structure/function studies described focused upon understanding how the topology and structures of the membrane anchor domains of PGIS and TXAS influence their enzyme functions and their coordination with upstream COX-1 or -2 in the biosynthesis of TXA_2 and PGI_2 in the native membrane-bound environment. The data summarized here are essentially generated by our research group.

*Address correspondence to this author at the Vascular Biology Research Center and Division of Hematology, Dept. of Internal Medicine, University of Texas Health Science Center at Houston, 6431 Fannin St., Houston, TX 77030, USA; Tel.: 713-500-6769; Fax: 713-500-6810; E-mail: kruan@uth.tmc.edu

1389-5575/04 $45.00+.00

2. MOLECULAR MODELING OF PGIS AND TXAS

It is believe that cytochrome P450 enzymes share similar backbones in protein folding evidenced by the structural similarity in the crystallographic structures known for several soluble bacterial P450s, including $P450_{cam}$ [19], $P450_{BM-3}$ [20] and $P450_{ter}$ [21], and an engineered microsomal P450 (P450 2C5) with deleted N-terminal membrane anchor domain and modified helix F/G loop [22,23]. Several 3D structural models of the catalytic domains of mammalian P450s have been constructed by homology modeling based on the crystal structures of the soluble P450s. $P450_{BM-3}$ is considered to be functionally and structurally related to the microsomal P450s including PGIS and TXAS [20,24], as reflected in their about 25% sequence identity and their substrate similarities. PGH_2, the substrate for PGIS and TXAS, is derived from AA that is also a substrate for $P450_{BM-3}$. Thus, the substrate binding cavities and docking sites of PGIS and TXAS are likely to have general structural features roughly similar to $P450_{BM-3}$. Thus, the x-ray structure of $P450_{BM-3}$ provides a useful template for PGIS and TXAS model construction. We have constructed working 3D structural models for human PGIS [25] (Fig. **2A**) and TXAS [24] (Fig. **2B**) based on the crystallographic structure of the $P450_{BM-3}$. The overall features of these 3D models of TXAS and PGIS have been supported by our site-directed mutagenesis of several important residues in the predicted substrate- and haeme-binding sites [25-26]. Recently, we have also constructed the 3D structural model of PGIS [27-29] and TXAS (data not published) using the engineered microsomal P450 2C5. One major limitation of the homology modeling for PGIS and TXAS was that they provided no structural information about the N-terminal membrane anchor structures and about the membrane topology because the soluble P450s and engineered P450 2C5 used as templates lack N-terminal membrane anchor domains [22-24,30]. The PGIS and TXAS models have played important roles to guide our experimental designs for the structural and functional characterization and topology studies of the synthases.

3. OVERALL MEMBRANE TOPOLOGY OF THE CATALYTIC DOMAINS OF PGIS AND TXAS

To understand the biosynthesis of PGI_2 and TXA_2 in the ER environment through coordination with COX, it is crucial to localize the catalytic domains of the synthases in respect to the ER membrane. Kinetic studies for PGIS and TXAS using several specific inhibitors with modified PGH_2 endoperoxide oxygen structures suggested that the C-9 endoperoxide oxygen of PGH_2 is likely to interact with the heme ferric iron of TXAS [31]. In contrast, the C-11 endoperoxide oxygen of PGH_2 interacts with the heme iron of PGIS [31]. This brings up interesting questions of how the protein structures and the membrane environment influence the substrate presentations differently in the synthases.

The overall membrane topology of microsomal P450s has been proposed to have two possible models: (a) the large catalytic domain exposed on the cytoplasmic side of the ER membrane with an N-terminal membrane anchor, or (b) deep immersion of the catalytic domain in the ER membrane [32]. To find out which membrane topological model is adopted by PGIS and TXAS, we have characterized the membrane topology of the catalytic portion of PGIS using site-specific antibodies targeted at specific protein segments identified as being surface-exposed by molecular modeling. The 3D working model of human PGIS, constructed by homology modeling using the $P450_{BM-3}$ crystal structure as

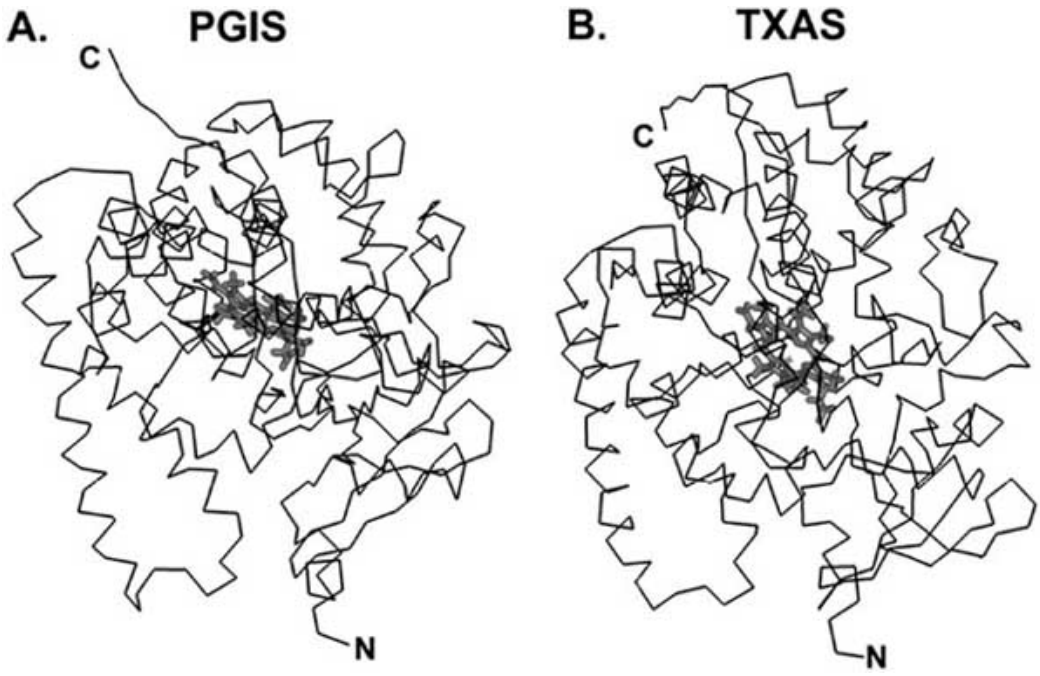

Fig. (2). Putative overall structural models of PGIS (A) and TXAS (B). The 3D structural working models were constructed by homology modeling using $P450_{BM-3}$ as a template [24,25]. The dark lines in the center of the models indicated heme. The N- and C-terminal positions were indicated with N and C respectively.

a template (Fig. **2A**), was used to design three hydrophilic peptides corresponding to different regions of the putative surface portion of PGIS, along with a N-terminal hydrophobic peptide (residues 1-28). Each peptide was synthesized and used to prepare the site-specific antibodies. All of the three antibodies against the putative surface segment of PGIS had high titer and specifically recognized human PGIS [33]. In contrast, the hydrophobic N-terminal peptide antibody had a much lower titer binding to the PGIS protein. The overall arrangement of the PGIS polypeptide with respect to the ER membrane was examined by immunocytochemistry in COS-1 cells transiently transfected with recombinant human PGIS cDNA and in ECV cells expressing endogenous PGIS [33]. The immunofluorescence staining for the cells with selective permeabilization of the plasma membrane using streptolysin O indicated that all of the three-peptide antibodies against the putative surface segments had access to their targets on the cytoplasmic side of the ER membrane. These results directly support both the structural model for PGIS based on $P450_{BM-3}$, in which the segments are located on the protein surface, and the membrane topology model in which PGIS has the bulk of the catalytic domain exposed on the cytoplasmic side of the ER membrane [33]. To test whether the catalytic domain of TXAS is similar to PGIS located on the cytoplasmic side of the ER, similar immunocytochemistry studies had been performed as described [33]. A putative surface segment (residues 373-390) predicted from the 3D structural model of TXAS, corresponding to the residues 353-368 of PGIS was synthesized and used for peptide antibody production. The site-specific antibody recognized TXAS protein with a high titer. The cell staining results indicated that the peptide antibody had access to its target on the cytoplasmic side of the ER membrane (data not shown). This information directly demonstrated that the localization of the segment of TXAS is likely similar to PGIS on the cytoplasmic side of the ER, and has led to propose a model for the topological arrangement of PGIS and TXAS coordinated with PGHS in the biosynthesis of PGI_2 and TXA_2 in the ER membrane as shown in Fig. **3**. In this "global" model, AA passes through the ER membrane, binds to COX-1 or -2 localized on the inside of the ER membrane and is converted into PGH_2 by the enzyme. And then the PGH_2 moved to the down stream synthases, PGIS or TXAS is through the ER membrane and binds to the catalytic sites of the synthases located on the cytoplasmic side, where it is converted to PGI_2 or TXA_2.

4. PRESENTATION OF THE PGH_2 TO PGIS AND TXAS FROM COX IN THE ER MEMBRANE

Despite the two isoforms, COX-1 and -2 have been crystallized and 3D structure were used to understand the topological arrangement on the ER membrane and the reaction mechanism of the conversion of AA to PGH_2, however, little information is available for the precise presentation of the COX product, PGH_2 to the downstream PGIS and TXAS at the structural level, particularly *in vivo*, in membrane bound environments. The findings of the topological arrangement of the catalytic domains of PGIS and TXAS shown in Fig. **3** have led us to hypothesize that: The ER membrane itself and membrane anchor domains of PGIS and TXAS are involved in coordination between COX and PGIS or TXAS. In the Fig. **3** model, whether the PGH_2 is presented to the synthase by directly crossing through the hydrophobic membrane or being exposed to the cytosol aqua and then moving into the binding side of the synthase is dependent on the orientation of the substrate access channel opening. Because the PGH_2 is not stable in polar environments, the paths of the hydrophobic membrane and polar medium in cytosol will make a difference in the rapid biosynthesis of PGI_2 and TXA_2 in response to the environment stimulation. Elucidation of their topological arrangement of the substrate channels of PGIS and TXAS in respect to the ER membrane is an important step to understand the path of PGH_2 presented to the synthases.

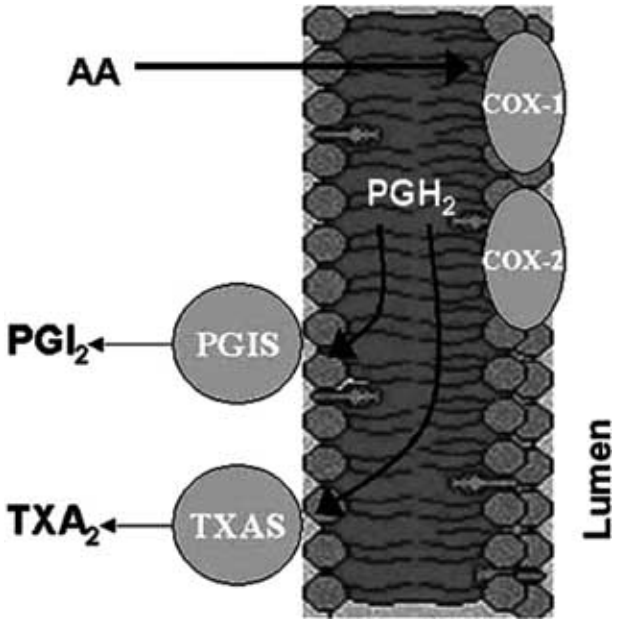

Fig. (3). The proposed location of the PGIS, TXAS, and COX-1 and -2 in respect to the ER membrane. The two synthases, PGIS and TXAS are likely to be at the cytoplasmic side of the ER membrane, which are opposite to the COX-1 and -2 located at the luminal side of the ER membrane.

The topology model having the large PGIS cytoplasmic domain anchored to the endoplasmic reticulum (ER) membrane by the N-terminal segment orients the substrate access channel opening to face the membrane. To test this orientation, we have explored the accessibility of the PGIS substrate channel opening to site-specific antibodies. The working 3D PGIS model, constructed by protein homology modeling (Fig. **2A**), was used to predict surface portions near the substrate access channel opening. Two peptides corresponding to the surface immediately near the opening [residues 66-75 (P66-75) and 95-116 (P95-116)], and two other peptides corresponding to the surface about 10-20 Å (1 Å=0.1 nm) away from the opening [residues 366-382 (P366-382) and 472-482 (P472-482)] were used to prepare site-specific antibodies. All four anti-peptide antibodies specifically recognized the synthetic segments of PGIS and recombinant human PGIS protein, as shown by binding assays and Western-blot analysis. The site-specific antibodies were used to probe the accessibility of the substrate access channel opening in transiently transfected COS-1 cells expressing recombinant human PGIS, and in spontaneously transformed human endothelial cell line ECV cells expressing endogenous human PGIS [34].

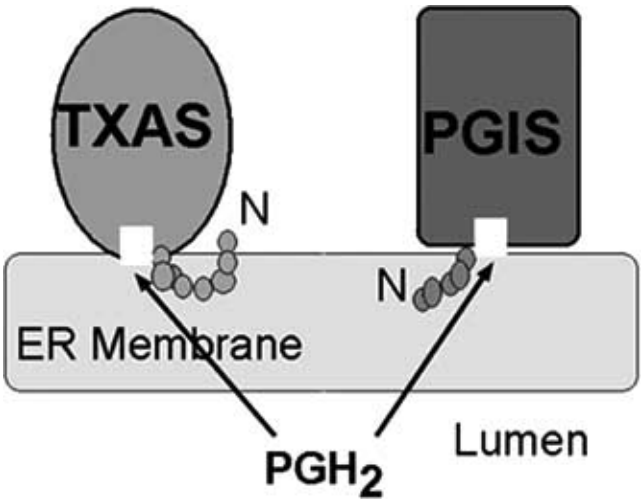

Fig. (4). The substrate access channel orientation of the PGIS and TXAS in respect to the ER membrane. The proposed substrate access channel opening of the PGIS and TXAS are positioned close to the ER membrane and covered by the membrane.

Immunofluorescence staining was performed for cells selectively permeabilized with streptolysin O and for cells whose membranes were permeabilized with detergent. Antibodies to peptides in the immediate vicinity of the substrate channel (P66-75 and P95-116) bound to their targets only after general permeabilization with Triton X-100. In contrast, the two antibodies to peptides further from the channel opening (P366-382 and P472-482) bound to their targets even in cells with intact ER membranes [34]. These observations support our topology model in which the PGIS substrate access channel opening is positioned close to the ER membrane (Fig. **4**). From these studies we concluded that the substrate access channel faces the ER membrane and is covered by the membrane. This raised the possibility that the bilayer itself forms part of the access channel. In this case, the PGIS lipophilic substrate, PGH_2, derived from AA by COX-1 or -2, would then have ready access to the substrate-binding site of PGIS without even leaving the membrane to contact the polar medium. This is consistent with the results from the studies of the relationship between the ER membrane and the substrate access channel for other P450s using hydrophobic drugs [35,36], and fluorescence energy transfer [37].

5. STRUCTURAL AND FUNCTIONAL STUDIES OF THE N-TERMINAL MEMBRANE ANCHOR DOMAINS OF PGIS AND TXAS

To more precisely define the orientation of the substrate access channel and the substrate presentation, it is important to identify the membrane anchor residues, and to test whether the hydrophobic membrane anchor residues and the membrane itself facilitates the substrate presentation.

The hydrophobic N-terminal domain of PGIS and TXAS were synthesized, and the secondary and 3D structures and membrane anchor residues had been characterized.

a. Secondary Structure and Membrane Anchor Function of the N-Terminal Domain of PGIS

PGIS and TXAS have only 16% amino acid sequence identity. Hydropathy analysis suggests that the putative N-terminal membrane anchor domain of PGIS is similar to many other membrane-bound microsomal P450s, which are thought to be anchored by a single transmembrane segment, and thus different from the TXAS anchor, which appears to have longer transmembrane segments [38]. To characterize the membrane anchor function of the PGIS N-terminal region, two overlapping peptides, mimicking putative N-terminal membrane anchor segments of PGIS were synthesized and their ability to insert in a lipid bilayer was evaluated. These peptides contain residues 1-28 (LP1) and residues 25-54 (LP2) of human PGIS. The results indicated that the LP1 peptide of PGIS became bound to the lipid bilayer, whereas the LP2 peptide could not bind to the lipid. The LP1 peptide was further characterized as to their conformation using CD spectroscopy. Helical structure was induced in the LP1 peptide by addition of trifluoroethanol (TFE), or dodecylphosphocholine (DPC), or by incorporation into liposomes**,** indicating that these segments tend to adopt a helical structure in a hydrophobic environment, and thus could function as membrane anchor segments [39]. Identical results were obtained by similar experiments using a well-characterised P450 2C1 as a control [39]. These results support that PGIS, like P450 2C1, appears to have a membrane anchor segment in the N-terminal region within the first 28 residues [39].

b. Solution Structure and Topology of the N-Terminal Membrane Anchor Domain of Prostaglandin I_2 Synthase

To further identify the membrane anchor residues in the N-terminal region, the solution structure of the PGIS LP1 peptide was determined by 2D ^{1}H NMR spectroscopy in TFE and DPC micelles, which mimic the hydrophobic membrane environment. A combination of 2D NMR experiments, including NOESY, TOCSY and double-quantum-filtered COSY, were used to obtain complete ^{1}H NMR assignments for the peptide. Using the NOE data obtained from the assignments and simulated annealing calculations; the solution structure of the N-terminal membrane domain was obtained. The PGIS N-terminal domain reveals a bent-shaped structure comprised of an

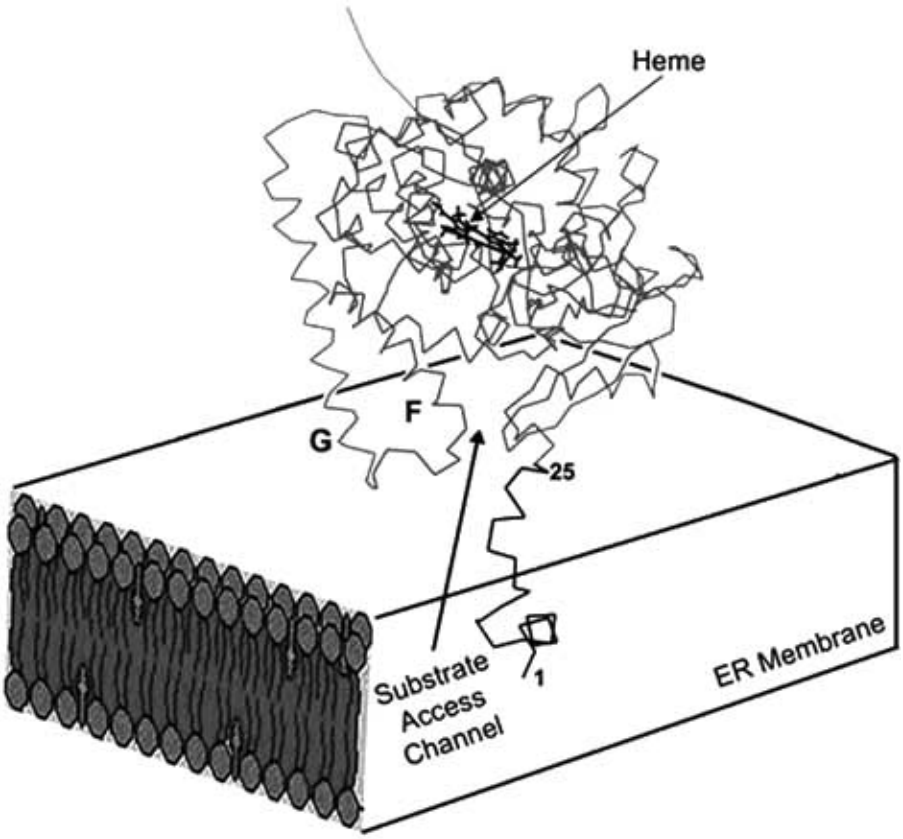

Fig. (5). Overall topology of the N-terminal membrane anchor domain of PGIS. The NMR 3D structure of residues 1-25 (dark line) of human PGIS was grafted on to a structural working model (backbone) constructed by homology modeling using $P450_{BM-3}$ as a template [24,25], and then inserted into the ER membrane with the first 20 hydrophobic residues [27]. The helix F/G loop was labeled with letters. The proposed substrate access channel was indicated with an arrow.

initial helix (residues 3-11), followed by a turn (residues 12-16) and a further atypical helix (residues 17-23) [27]. The hydrophobic side chains of the helix and turn segments (residues 1-20) are proposed to interact with the hydrocarbon interior of the phospholipid bilayer of the ER membrane. The hydrophilic side chains of residues 21-25 (Arg-Arg-Arg-Thr-Arg) point away from the hydrophobic residues 1-20 and are expected to be exposed to the polar environment on the surface of the ER membrane on the cytoplasmic side. The distance between residues 1 and 20 is approximately 20 Å, which is less than the thickness of the lipid bilayer (Fig. **5**). This indicates that the N-terminal membrane anchor domain of PGIS may not penetrate the ER membrane. The membrane anchor segment features in the N-terminal domains of other microsomal P450s may be similar to PGIS. Thus, the first NMR solution structure of the N-terminal domain is not only for PGIS, but also serves as a reference structure for other microsomal P450 superfamily members since no crystal structure for the N-terminal membrane anchor domain is available for any microsomal P450 enzyme.

6. STRUCTURE AND MEMBRANE CONTACT FUNCTION OF THE PGIS HELIX F/G LOOP

It has been reported that by simply removing the N-terminal domain of the microsomal P450s, the enzymes still associated with the membrane. Larson et al [40] expressed rabbit liver P450 2E1 in E. coli and found that the enzyme was localized to the inner membrane even when residues 3-29 were deleted. Yabusaki et al [41] obtained similar results when residues 1-30 were removed from a P450 expressed in yeast. These results suggest that the residues 1-30 at the N-terminus for the microsomal P450 enzymes are not the only membrane anchor component in the protein. Our working models for overall membrane topology of PGIS and TXAS have suggested that the helix F/G loop (corresponding to the helix F/G loop of the crystal structure of $P450_{BM-3}$) may contact the ER membrane (Fig. **2**). This interaction might explain why the deletion of the N-terminal membrane anchor regions of TXAS [42,43] and other microsomal P450s [40,41] did not release the proteins from the membrane. Direct support for the interaction of the F/G loop with the membrane comes from recent crystallography studies, in which modification of the F/G loop residues in a microsomal P450 enzyme, P450 2C5, lacking N-terminal residues 3-21, resulted in a soluble form which could be crystallized without using detergent [22,23]. In our PGIS and TXAS models, the helix F/G loops are in a position to influence the orientation of the substrate access channel with respect to the ER membrane (Fig. **2**). Thus, characterization of the membrane contact function of the helix F/G loop has become a key step in further defining the PGIS and TXAS membrane topologies and substrate channel orientations, along with determining the influences of the F/G loop on the enzyme catalytic activity.

a. Identification of the Residues Contacted with the ER Membrane in the Helix F/G Loop of PGIS

To provide direct experimental data to see whether the helix F/G loop of PGIS contains a membrane contact region distinct from the N-terminal membrane anchor domain, we have explored the relationship between the ER membrane and the PGIS helix F/G loop using high resolution 2D NMR spectroscopy and spine labeled technique. Using the distance between the F/G helix measured from the PGIS model as a guide, the helix F/G loop was mimicked in a synthetic peptide by introducing a spacer to maintain the distance of about 7 Å (PGIS residues 208 and 230). The synthetic peptide was constrained on both ends through a disulfide bond with added Cys residues [28]. The orientation and the residues contacted with the membrane of the PGIS F/G loop were evaluated from the effect of incorporation of a spin-labeled 12-doxylstearate into the center position of the DPC micelles in the present of the peptide using 2D ^{1}H NMR spectroscopy. The proton resonances of three residues in the peptide inserted into the DPC micelles were clearly perturbed by the paramagnetic effect of the spin labeled compound in the micelles. The three residues demonstrated to be incorporated into the DPC micelles in the peptide are corresponding to the PGIS residues, L217, L222 and V224 [28]. These results indicated that the residues are involved in contact with the ER membrane in the native membrane-bound PGIS. These studies provided the first experimental evidence localizing the membrane contact residues in the helix F/G loop region of the microsomal P450 and are valuable to further define the membrane topology of PGIS and those of other microsomal P450s in the native membrane environment.

b. Solution Structure of the Helix F/G Loop of PGIS

To demonstrate the membrane contacts of the F/G loop region in the native PGIS in 3D structural terms, the solution structure of the constrained PGIS F/G loop peptide was also determined. High-resolution ^{1}H 2D NMR experiments including TOCSY, DQF-COSY and NOESY spectra were collected for the F/G loop. Through the combination of 2D NMR experiments in the presence of DPC micelles used to mimic the membrane environment, complete ^{1}H NMR assignments of the F/G loop segment were obtained and the solution structure of the peptide was determined. The PGIS F/G loop segment shows a defined helix turn helix conformation, which is similar to the 3D crystallography structure of $P450_{BM-3}$ in the corresponding region. The identified membrane contacted residues in the F/G loop of PGIS were highlighted when the 3D structure of the F/G loop peptide was adopted into the 3D working model bound to the ER membrane. The substrate access channel is stabilized by the L217, L22 and V224 in the F/G loop and the first 20 hydrophobic residues in the N-terminal domain of the PGIS (Fig. **6**). The orientation of the substrate access channel favors adopting the lipophilic

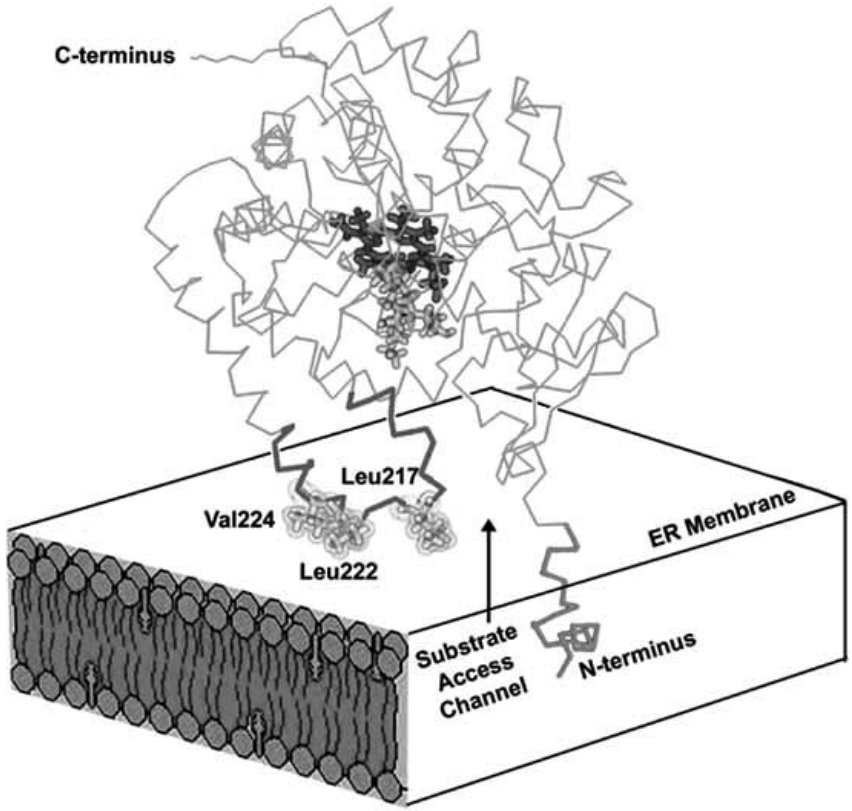

Fig. (6). Configuration of the NMR structure of the PGIS F/G loop relative to the PGIS 3D structural working model (residues 1-500), which was constructed as described in Fig. **5**. The NMR structure of the F/G loop (dark bold line) and the N-terminal segment (light bold line) were grafted to the corresponding region of the model. The side chains of the residues (Leu217, Leu222, Val224) within the F/G loop in contact with the ER membrane were shown. Heme (dark) and substrate (light) were displayed in the center of the model [28].

substrate, PGH_2, into the binding site of PGIS from the membrane in a highly efficiency way.

7. MEMBRANE ANCHOR REGIONS ARE INVOLVED IN SUBSTRATE PRESENTATION

As the model shows in Fig. **5**, the hydrophobic membrane anchor residues in the N-terminal and the F/G loop region are highly probable to be involved for the substrate presentation. To test this hypothesis, we have explored an approach to identify the residues in the N-terminal and the helix F/G loop domains important to the catalytic function of the membrane-bound PGIS and TXAS by 2D NMR experiment and mutagenesis methods.

The first evidence showing the interaction between the substrate and the membrane anchor domains was shown by the interaction between the TXAS N-terminal domain and the PGH_2 analog, U44069 in a membrane environment using high resolution 2D NMR spectroscopy studies [44]. A synthetic peptide corresponding to the N-terminal membrane anchor domain (residues 1-35) of TXAS, which adopted a stable helical structure and exhibited a membrane anchor function in the membrane-bound environment identified by CD spectroscopy, was used to interact with a stable PGH_2 analog, U44069. 2D ^1H NMR experiments, NOESY and TOCSY, were performed to solve the solution structures of U44069 in a membrane-mimicking environment using DPC micelles. Completed ^1H NMR assignments were obtained, and the data were used to construct 3D structures of the PGH_2 analog in DPC micelles, showing the detailed conformation change upon the interaction with the membrane anchor domain. Different conformations of U44069 were clearly observed in the presence and absence of the TXAS N-terminal membrane anchor domain. This observation supported the presence of a substrate interaction site in the N-terminal region of TXAS. This implied that the presentation of PGH_2 to the binding site of the membrane-bound TXAS through the substrate access channel can be influenced/modulated by the N-terminal membrane domain.

Very recently, the constrained F/G loop peptide of PGIS was used to interact with the enzyme substrate analogue, U46619 (another stable PGH_2 mimic). High-resolution 2D NMR experiments were performed to determine the contacts between the F/G loop peptide and U46619. The interaction was confirmed by the observation of the conformational changes of the peptide and U46619 using the comparison of the cross-peaks between the NOESY spectra of U46619 with the peptide, without the peptide, and the peptide alone. Through the combination of the 2D NMR experiments, completed ^1H NMR assignments of the F/G loop segment in the presence and absence of U46619 were obtained, and the intermolecular NOEs were used to predict the contact residues (Leu214 and Pro215) of the F/G loop with the PGIS substrate. The predicted influence of residues on enzyme catalytic activity in membrane-bound environments was further confirmed by the site-directed mutagenesis of the F/G loop residues of human PGIS [29]. The observations supported that the F/G loop is involved in forming the substrate access channel for membrane-bound PGIS and that the substrate presentation to the binding site of the membrane-bound synthase could be influenced/modulated by the F/G loop residues (Fig. **7**).

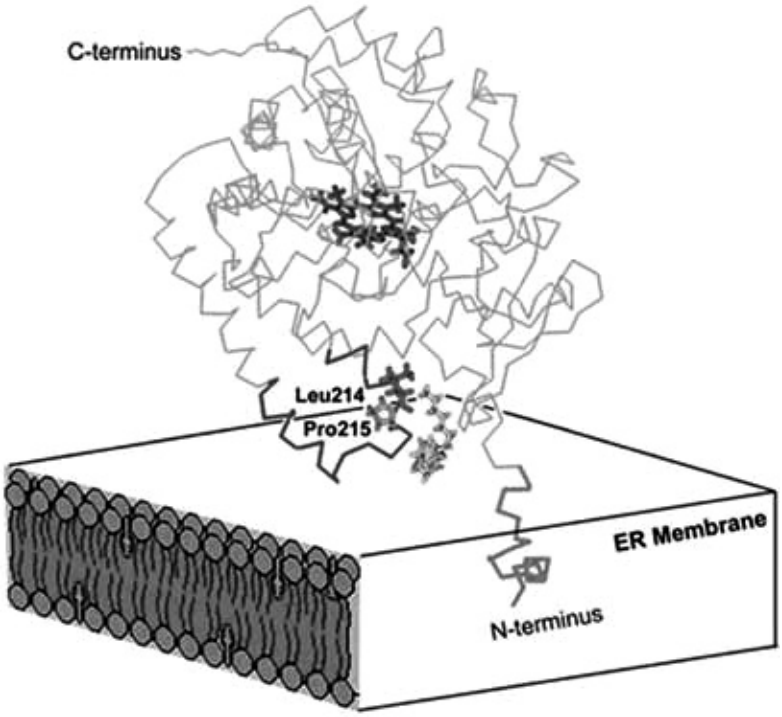

Fig. (7). Refined topological model of the native PGIS in respect to the ER membrane with the NMR structures of the bound form of F/G loop (dark bold line) and the N-terminal segment (light bold line) connected. The side chain of the identified residues (Leu214 and Pro215) that contacted with U46619 were displayed. U46619 was placed in the position of the substrate access channel based on the data from the NMR experiments [29]. Heme was displayed in the center of the model.

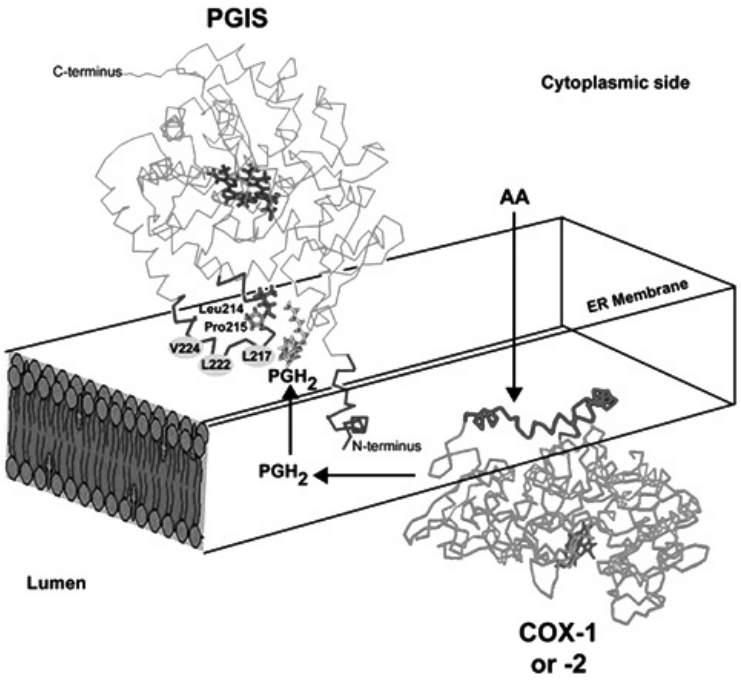

Fig. (8). A model of the coordination of PGIS and COX in the biosynthesis of PGI_2 in the ER membrane.

8. COORDINATION OF PGIS OR TXAS AND COX IN THE BIOSYNTHESIS OF PGI_2 AND TXA_2 IN THE ER MEMBRANE

Crystallographic studies of detergent-solubilized COX-1 and -2 suggest that the catalytic domains of the proteins lie on the lumenal side of the ER, anchored to the ER membrane by hydrophobic side chains of amphipathic helices A-D (Fig. **8**). These hydrophobic side chains of the membrane anchor domains also form an entrance to the substrate-binding channel and potentially form an initial docking site for the lipid substrate, AA [45,46]. The topology models, developed from the above studies, of PGIS and TXAS, have their proteins localized on the cytoplasmic side of the ER and the substrate access channel entrances opened to the ER membrane. The inside-by-outside arrangement in the ER membrane for COX and PGIS/TXAS reflects that their coordination in the biosynthesis of PGI_2 and TXA_2 is facilitated by the enzyme's anchoring in the lipid membrane and the ER membrane itself (Fig. **8**). This suggested that the efficiency of eicosanoid biosynthesis will be different in the soluble and the membrane-bound enzymes. One indication of such differences has been reported from Eling et al [47] who found channeling of AA through prostaglandin G_2 (PGG_2) to PGH_2 in microsomal PGHS, but not in detergent-solubilized PGHS. Another observation, which supports this hypothesis, is that COX side products are much less plentiful in the biosynthesis of PGI_2 and TXA_2 with intact membrane-bound systems as compared to solubilized enzymes. This suggests that the lipid substrates, AA and PGH_2, have higher-efficiency access to the active sites, and less chance to be degraded, in the membrane-bound system compared to the cytosol aqueous system. The details of the coordination between the COX enzymes with PGIS/TXAS in the ER membrane, which includes the physical contact of the synthases, dynamic changes of the topological arrangement of the synthases and the different PGH_2 presentations between the membrane bound PGIS and TXAS, remain challenging in the eicosaniod biosynthesis studies.

9. CONCLUSIONS

Overall, the information described above included that: a. 3D structural working models of human PGIS and TXAS constructed by molecular modeling using $P450_{BM-3}$ and 2C5 as templates could be used as initial guides to design experiments for structural and functional studies of the synthase; b. Catalytic domains of PGIS and TXAS are localized on the cytoplasmic side of the ER membrane; c. The substrate access channel of PGIS faces toward and is in contact with the ER membrane; d. The 3D solution structures of the N-terminal and F/G loop domains of PGIS in membrane-bound environments have been solved; e. The membrane anchor residues within the N-terminal domain and F/G loop have been identified; f. The residues within the N-terminal membrane region of TXAS and in the F/G loop that influenced the substrate presentation have been determined; g. The presentation of PGH_2 from COX to downstream PGIS or TXAS is within the ER membrane. These findings have provided a great advancement in our understanding the biosynthesis of PGI_2 and TXA_2 in the native ER membrane via COX pathway at cellular and submolecular levels and provide the structural basis in the synthase engineering for the next generation gene therapy and drug designs specifically targeting the biosynthesis of PGI_2 and/or TXA_2 in vivo.

ACKNOWLEDGEMENTS

I thank Dr. Xiaolian Gao in the Chemistry Department, University of Houston, for access to the NMR facility and

providing valuable advice on taking the NMR Spectra. I also thank Lori Jenkins and Alice So for the manuscript editing assistance.

NOTE

This work was supported by National Institutes of Health Grants HL 56712 and NS 23327.

ABBREVIATIONS

The abbreviations used are: TXA_2, thromboxane A_2; NOESY, nuclear Overhauser effect spectroscopy; TOCSY, total correlation spectroscopy; HPLC, high performance liquid chromatography; DQF-COSY, double-quantum filtered correlation spectroscopy.

REFERENCES

[1] Majerus, P.W. *J. Clin. Invest.*, **1983**, *72*, 1521-1525.
[2] Miller, D.K.; Sadowski, S.; Soderman, D.D.; Kuehl, F.A. Jr. *J. Biol. Chem.*, **1985**, *260*, 1006-1014.
[3] Smith,W.L. *Annu. Rev. Physiol.*, **1986**, *48*, 251-262.
[4] Needleman, P.; Turk, J.; Jackschik, B.A.; Morrison, A.R.; Lefkowith, J.B. *Annu. Rev. Biochem.*, **1986**, *55*, 69-102.
[5] Granstrom, E.; Diczfalusy, U.; Hamberg, M.; Hansson, G.; Malmsten, C.; Samuelson, B. In *Prostaglandins and the cardiovascular system*; Oates, J.A., Ed; Raven Press, New York, **1982**; pp. 15-58.
[6] Bunting, S.; Gryglewski, R.; Moncada, S.; Vane J.R. *Prostaglandins*, **1976**, *12*, 897-913.
[7] Moncada, S.; Herman, A.G.; Higgs, E.A.; Vane, J.R. *Thromb. Res.*, **1977**, *11*, 323-344.
[8] Weksler, B.B.; Ley, C.W.; Jaffe, E.A. *J. Clin. Invest.*, **1978**, *62*, 923-930.
[9] Ingerman-Wojenski, C.; Silver, M.J.; Smith, J.B.; Macarak, E. *J. Clin. Invest.*, **1981**, *67*, 1292-1296.
[10] Smith, W.L.; DeWitt, D.L.; Allen, M.L. *J. Biol. Chem.*, **1983**, *258*, 5922-5926.
[11] Ohashi, K.; Ruan, K.-H.; Kulmacz., R.J.; Wu, K.K.; Wang, L.-H. *J. Biol. Chem.*, **1992**, *267*, 789-793.
[12] Yokoyama, C.; Miyata, A.; Ihara, H.; Ullrich, V.; Tanabe, T. *Biochem. Biophys. Res. Commun.*, **1991**, *178*, 1479-1484.
[13] Shen, R.-F.; Back, S.J.; Zhang, L.; Chase, M.B.; Tai, H.-H.; Purtell, D.C. Eighth Int. Conf. on prostaglandins and related compounds. **1982.** Cloning, expression, and chromosomal mapping thromboxane synthase.
[14] Pereira, B.; Wu, K.K.; Wang, L.-H. *Biochem. Biophys. Res. Commun.*, **1994**, *203*, 59-66.
[15] Miyata, A.; Hara, S.; Yokoyama, C.; Inoue, H.; Ullrich, V.; Tanabe, T. *Biochem. Biophys. Res. Commun.*, **1994**, *200*, 1728-1734.
[16] Haurand, M.; Ullrich, V. *J. Biol. Chem.*, **1985**, *260*, 15059-15067.
[17] Ullrich, V.; Castle, L.; Weber, P. *Biochem. Pharmacol.*, **1981**, *30*, 2033-2036.
[18] Ullrich, V.; Graf, H. *Trends Pharmacol. Sci.*, **1984**, *5*, 352-355.
[19] Poulos, T.L.; Finzel, B.C.; Howard, A.J. *J. Mol. Bio.*, **1987**, *195*, 697-700.
[20] Ravichandran, K.G.; Boddupalli, S.S.; Hasermann, C.A.; Peterson, J.A.; Deisenhofer, J. *Science*, **1993**, *261*, 731-736.
[21] Boddupalli, S.S.; Hasemann, C.A.; Ravichandran, K.G.; Lu, J.Y.; Goldsmith, E.J.; Deisenhofer, J.; Peterson, J.A. *Proc. Natl. Acad. Sci. USA*, **1992**, *89*, 5567-5571.
[22] Williams, P.; Sridhar, V.; McRee, D.E. 11th International Conference on Cytochrome P450, Sendai, Japan, **1999**, pp. 19, L3.
[23] Johnson, E.F.; Cosme, J.; Williams, P.; McRee, D.E. *11th International Conference on Cytochrome P450, Sendai, Japan*, **1999**, pp. 18, L2.
[24] Ruan, K.-H.; Milfeld, K.; Kulmacz, R.J.; Wu, K.K. *Protein Eng.*, **1994**, *7*, 1345-1351.
[25] Shyue, S.-K.; Ruan, K.-H.; Wang, L.-H.; Wu, K.K. *J. Biol. Chem.*, **1997**, *272*, 3657-3662.
[26] Wang, L.-H.; Matijevic-Aleksic, N.; Hsu, P.Y.; Ruan, K.-H.; Wu, K.K.; Kulmacz, R.J. *J. Biol. Chem.*, **1996**, *33*, 19970-19975.
[27] Ruan, K.-H.; So, S.-P.; Zheng, W.; Wu, J.; Li, D.; Kung, J. *Biochem. J.*, **2002**, *368*, 721-728.
[28] Wu, J.; So, S.P.; Ruan, K.-H. *Arch Biochem. Biophys.*, **2003**, *411*, 27-35.
[29] Deng, H.; Wu, J.; So, S.P.; Ruan, K.H. *Biochemistry*, **2003**, *42*, 5609-5617.
[30] Zvelebil, M.J.; Wolf, C.R.; Sternberg, M.J.E. *Protein Eng.*, **1991**, *4*, 271-282.
[31] Hecker, M.; Ullrich, V. *J. Biol. Chem.*, **1989**, *264*, 141-150.
[32] Miller, J.P.; Herbette, L.G.; White, R.E. *Biochemistry*, **1996**, *35*, 1466-1474.
[33] Lin, Y.Z,; Deng, H.; Ruan, K.H. *Arch. Biochem. Biophys.*, **2000**, *379*, 188-197.
[34] Deng, H.; Huang, A.; So, S.P.; Lin, Y.Z.; Ruan, K.H. *Biochem. J.*, **2002**, *362*, 545-551.
[35] Al-Gailany, K.A.; Houston, J.B.; Bridges, J.W. *Biochem. Pharmacol.*, **1978**, *27*, 783-788.
[36] Parry, G.; Palmer, D.N.; Williams, D.J. *FEBS Lett.*, **1976**, *67*, 123–129.
[37] Centeno, F.; Guiterrez-Merino, C. *Biochemistry*, **1992**, *31*, 8473–8481.
[38] Ruan, K.-H.; Li, P.; Kulmacz, R.J.; Wu, K.K. *J. Biol. Chem.*, **1994**, *269*, 20938-20942.
[39] Lin, Y.; Wu, K.K.; Ruan, K.H. *Arch. Biochem. Biophys.*, **1998**, *352*, 78-84.
[40] Larson, J.R.; Coon, M.J.; Porter, T.D. *J. Biol. Chem.*, **1991**, *266*, 7321-7324.
[41] Yabusaki, Y.; Murakami, H.; Sakaki, T.; Shibata, M.; Ohkawa, H. *DNA*, **1988**, *7*, 701-711.
[42] Xia, Z.; Tai, H.H. *Arch. Biochem. Biophys.*, **1995**, *321*, 531-534.
[43] Hsu, P.Y.; Tsai, A.L.; Kulmacz, R.J.; Wang, L.-H. *J. Biol. Chem.*, **1999**, *274,* 762-769.
[44] So, S.P.; Li, D.; Ruan, K.H. *J Biol Chem.*, **2000**, *275*, 40679-40685.
[45] Pico, D.; Loll, P.J.; Garavito, R.M. *Nature*, **1994**, *367*, 243-249.
[46] Kurumbail, R.G.; Stevens, A.M.; Gierse, J.K.; Mcdonald, J.J.; Stegeman, R.A.; Pak, J.Y.; Gildehaus, D.; Miyashiro, J.M.; Penning, T.D.; Seibert, K.; Isakson, P.C.; Stallings, W.C. *Nature*, **1996**, *384*, 644-648.
[47] Eling T.E.; Glasgow, W.C.; Curtis, J.F.; Hubbard, W.C.; Handler, J. A. *J. Biol. Chem.*, **1991**, *266*, 12348-12355.